Local organization and atomic clustering in multicomponent amorphous steels

V. Yu. Kazimirov,[1] Despina Louca,[1] M. Widom,[2] X.-J. Gu,[1] S. J. Poon,[1] and G. J. Shiflet[3]
[1]*Department of Physics, University of Virginia, Charlottesville, Virginia 22904, USA*
[2]*Department of Physics, Carnegie Mellon University, Pittsburgh, Pennsylvania 15213, USA*
[3]*Department of Materials Science and Engineering, University of Virginia, Charlottesville, Virginia 22904, USA*
(Received 2 July 2008; revised manuscript received 24 July 2008; published 15 August 2008)

The characteristics of atom packing in multicomponent metallic alloys with distinct short- and medium-range order (SMRO) are notoriously difficult to provide as the local structure is made up of multiple overlapping pair correlations. In the case of binary glasses, several cluster models have been proposed that can describe the SMRO well going beyond models of dense random packing of hard spheres. By combining the pair density function analysis of neutron-diffraction data and modeling using *ab initio* computational techniques, the tendency for local atomic clustering is investigated and properties of multicomponent bulk $Fe_{78-x-y}TM_xRE_y(C_{22-z}B_z)$ amorphous alloys [transition metal (TM) and rare earth (RE)] are studied going beyond simple binary systems. The results are relevant to most bulk metallic glass forming alloys with more than one kind of solute ion.

DOI: 10.1103/PhysRevB.78.054112 PACS number(s): 61.43.−j, 61.05.F−, 64.70.Q−

The discovery of bulk noncrystalline metallic alloys with improved glass forming ability and unique properties[1–5] has opened the possibility for commercial applications, as well as renewed the interest toward understanding the nature of the glass and glass transition. In spite years of research in this field, the details of local atomic organization and fluctuations are poorly understood. The local atomic structure of amorphous metals is commonly thought of as a superposition of single-atom coordination environments, yielding a well-defined short-range order that strongly depends on chemical composition.[6,7] The building blocks for constructing such an amorphous topology are derived from an infinite variation of local atomic environments, where individual atoms (even of the same chemical species) can be in unique neighborhoods because of minute variations in the type of neighboring atoms. Naively, we can assume that in order to reproduce the structure and atomic properties of metallic glasses, at least 10^{23} types of local environments are needed to be treated independently, which is an impossible task. With such a many-body problem at hand combined with the lack of translational symmetry and the absence of a descriptive unit cell, as found in the case of crystals that can be used to reproduce the three-dimensional structure in space, resolving the glass structure and determining the geometrical arrangement of atoms becomes immensely difficult. To this end, we will apply experimental and computational techniques to probe the collective behavior of atoms in an attempt to provide insights into the nature of the atomic topology and clustering tendencies of multicomponent Fe glasses going beyond binary systems.

To provide a realistic description of the three-dimensional structure of metallic glasses and associate the coordinated environment of atoms to physical properties, the first-principles quantum-mechanical (*ab initio*) molecular-dynamics (MD) method[8–10] along with the pair density function (PDF) (Refs. 11–14) analysis of diffraction data are used to consider the role of chemical effects, ionic size ratios, and concentration. Currently, *ab initio* techniques are widely used for the investigation of crystals and ordinary silicate glasses with predominantly covalent type of bonding. The *ab initio* technique has strict limitations on the model size because it is computationally intensive. Until recently, only a few simple binary alloys[15,16] have been studied although, in other disciplines, more complex polymeric molecules and even proteins have been successfully described by *ab initio* methods.[17,18] To apply this approach to complex multicomponent metallic alloys, it is important to explore whether the use of a relatively small number of atoms in a model system with periodic boundary conditions and an imposed rapid quenching are sufficient to describe the main structural characteristics of complex glasses. At the same time, classical MD and reverse Monte Carlo methods are widely used to describe atomic structures and physical properties of glasses. However classical MD makes use of semiempirical potentials, while the parameters for the potentials are defined through fitting to experimental data and are unique to each particular system. This essentially restricts the application of classical MD as a predictive tool. This problem is exacerbated in the case of multicomponent alloys where the number of different pair correlations goes to the order of $N(N-1)$, where N is the number of distinct chemical species. Moreover, the total energy in metallic glass systems cannot be described by a simple sum of all pair potentials. Additional terms related to energy exchange between free electrons and the nuclear subsystem must be introduced in the Hamiltonian, which is not a trivial process. In contrast, the *ab initio* MD based on density-functional theory does not have these limitations, makes use of no adjustable parameters, and accounts for electron interactions physically based on first quantum-mechanical principles. Thus, *ab initio* MD represents a unique tool for studying multicomponent metallic glasses.

The analysis of chemically distinct amorphous alloys of Fe-TM-RE-ME (TM=transition metals such as Mn, Cr, and Mo; RE=rare-earth ions such as Er and Y; and ME =metalloid ions such as C and B) with varying amounts of TM, RE, and ME demonstrated that the experimentally determined local atomic structure can be reproduced with very good accuracy using a model consisting of 100 atoms. The chemical coordination environment around each atom can be

determined from which cluster structures that give rise to the local order of the first and second coordination spheres can be identified. The local structure is simulated through the solid-liquid transition, which shows how short-range correlations are preserved well into the liquid phase. The atomic mean-square displacements are estimated to be large for light elements such as C and B and small for heavier elements such as Er. At the same time, the rate at which the displacements change differs with the chemical composition. Simultaneously, physical quantities, such as the bulk modulus, can be obtained and show that the values agree quite well with those obtained experimentally.

The alloys were synthesized following the procedure described in Refs. 19 and 20. Both ribbons and rods were used for the diffraction experiments. The neutron experiments were carried out using the neutron powder diffractometer at the Manuel Lujan Neutron Science Center of Los Alamos National Laboratory and the special environment powder diffractometer of the Intense Pulsed Neutron Source of Argonne National Laboratory. The total scattering structure function obtained from the diffraction data after correcting for multiple and inelastic scattering, absorption, and instrumental background was Fourier transformed to obtain the PDF. The PDF analysis provides a real-space representation of atomic pair correlations without assuming structural periodicity. It is particularly suited to the investigation of disordered or partially disordered systems.[21]

The simulations were carried out using the Vienna *ab initio* simulation package[22] together with the projector-augmented wave method. In order to properly reproduce magnetization effects, the Perdew-Wang generalized gradient approximation exchange-correlation functional with Vosko-Wilk-Nusair spin interpolation was used instead of the local-density approximation (LDA). The calculations for temperatures below 1500 K were performed with collinear spin polarization on Fe atoms. This was done to simulate the role of localized magnetic moments and can be important even in the liquid state. Monkhorst-Pack grids contained only the Γ point for simulated liquid and amorphous cells. The time step in the MD simulations was 1 fs. Since the LDA does not work for *f* electrons in rare earths, the potential for Er keeps the *f* electrons "frozen" in the pseudopotential core. The metastable phase of $Fe_{23}C_6$ was chosen as the initial structure. This phase is usually present as a competing crystalline phase[20,23,24] during the quenching process. Fe and C atoms from $Fe_{23}C_6$ were randomly substituted with different chemical elements to acquire the right chemical composition of the alloy to be simulated. The model consisted of 100 atoms in a cubic box with dimensions of $\sim 10 \times 10 \times 10$ Å^3 and periodic boundary conditions were used. The preliminary MD calculations were conducted at temperatures as high as 2000 K to allow atoms to diffuse and "forget" their initial positions in addition to allowing for a more realistic atomic arrangement for chemically distinct glasses.

Figure 1(a) is a plot of the experimental PDF corresponding to the local atomic structure of three bulk Fe glasses with different chemical compositions and ionic size ratios. Starting from Fe-Mo-C-B, when an additional solute ion is introduced such as Cr and Y, the short- and medium-range structures change in the way shown in the figure. Most clear

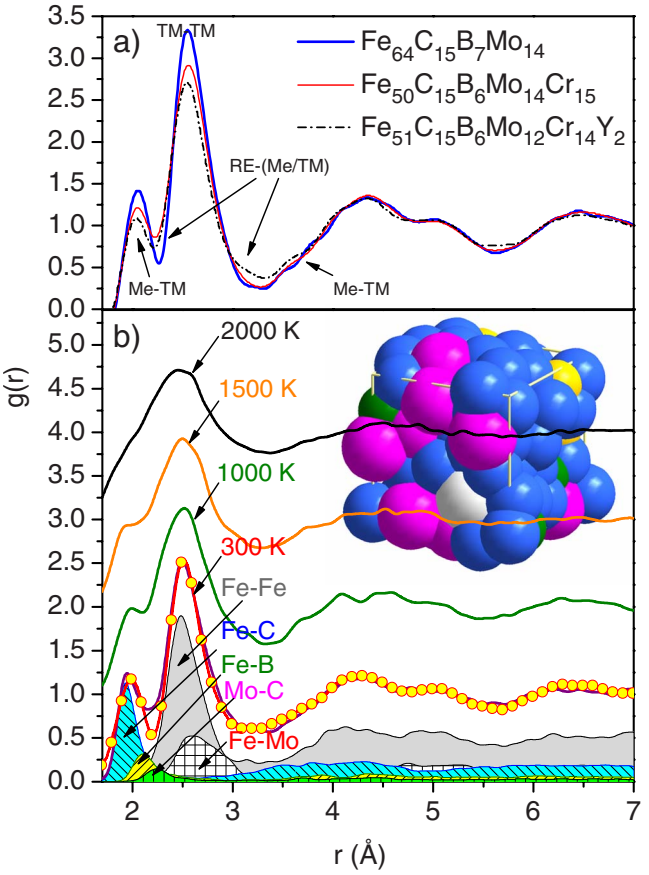

FIG. 1. (Color online) (a) The experimental pair distribution function $g(r)$ of the listed alloys at room temperature. These were determined from neutron-diffraction data. (b) Comparison of the experimental PDF (symbols) of $Fe_{63}Mo_{14}C_{15}B_6Er_2$ to the simulated PDF (line) obtained from the *ab initio* calculation of the structure shown in the inset of (b). Also shown in the figure are select partial functions of pairs of atoms (not shown are pairs with very small contributions). The simulated structure is additionally plotted as a function of temperature. Note that the short-range correlations remain well into the liquid state.

differences are observed up to 4 Å. Since the atoms do not reside at specific sites in the solid, the local structure peaks can be preliminary assigned by considering nominal values of atomic radii[25] and these are indicated in the figure. Thus the first peak corresponds to the TM-C/B pairs, which changes as Fe is substituted with Cr and Y. Very close to this peak are contributions from Y/Mo-ME pairs. The second peak is due to Fe-Fe followed by Fe-Mo/Y pair correlations and its position and shape changes based on the atom size and concentration. For subsequent peaks, assignments cannot be made by simply considering atomic radii because it becomes increasingly difficult to identify bond distances between second- and third-nearest neighbors. For distances beyond 7 Å, the atom-atom correlations become even less well defined and the PDF has no characteristic features. For this reason, a model is needed that can describe the atomic structure beyond nearest neighbors.

In Fig. 1(b), the experimental PDF of $Fe_{63}Mo_{14}C_{15}B_6Er_2$ (solid symbols) is compared to a model PDF (solid line) for the simulated structure of the same compound. The particular

model used is shown in the inset. It is apparent that agreement between the two PDFs is quite good: peak positions, shapes, and intensity are reproduced well. Since the model size is small and periodic boundary conditions are used, a spurious PDF peak appears at relatively high distances at about 10 Å. Similar agreements were obtained for the other alloys of which experimental PDFs are shown in Fig. 1(a). Select partial PDFs modeled by *ab initio* MD are also shown in the figure that help to identify the various atom-atom contributions in real space. Note that the area under the peaks is proportional to the concentration and the neutron-scattering length of each element in the chemical formula. It can be seen that Fe-C pairs are slightly shorter than Fe-B pairs and this may be significant in forming stronger Fe-C bonds. At the same time, Mo-C pairs are longer while Mo-B pairs are even longer but the contribution of the latter is too weak to show in the figure. Clearly, the Fe-Fe pairs dominate the PDF. Also shown in Fig. 1(b) is the evolution of the simulated structure as a function of increasing temperature. Up to ~1500 K, the Fe-C/B peak is discernibly distinct from the main Fe-Fe peak. Beyond that, the features become broad as the alloy melts but the structure retains some of the very short pair correlations well into the liquid state. The Fe-C/B peak has by now merged with the Fe-Fe peak forming a cluster of atoms with a finite distribution of bond correlations that are not spread out everywhere in real space.

An important aspect to understanding glass-forming ability and stability is atomic diffusion. In particular, slow atomic diffusion may lead to better glass-forming ability by reducing the critical quenching rate. Atom displacements of different chemical species should be studied as a function of time t in order to simulate diffusion and the value of the MD time window becomes a critical parameter in estimating values of diffusion coefficients. In the case of classical MD, the time window can be as large as a μs; but in the case of *ab initio* MD, the time window is at most several picosecond because the calculations are computationally expensive. For this reason, only the atomic mean-square displacements $\langle r(t)^2 \rangle$ are obtained as a function of t at temperatures in the liquid phase as they can provide qualitative information on how the different chemical species evolve with time and with different chemical environments. This is shown in Fig. 2 for $Fe_{49}B_6C_{15}Mo_{14}Er_1Cr_{15}$ and $Fe_{79}C_{15}B_6$ at $T=2000$ K. At short times, $\langle r(t)^2 \rangle$ grows quadratically as $(3k_BT/M)t^2$ corresponding to ballistic (without scattering) motion of the atom. As the structure relaxes at longer time scales, $\langle r(t)^2 \rangle$ demonstrates a nearly linear behavior. It can be seen that light elements such as C and B undergo large displacements while heavier elements are much slower—the slowest being Er. However, the $\langle r(t)^2 \rangle$ for C, B, and Fe are different in the two compounds, indicating that these ions diffuse much faster in $Fe_{79}C_{15}B_6$ than in $Fe_{49}B_6C_{15}Mo_{14}Er_1Cr_{15}$. It can also be seen that B diffuses faster than C in $Fe_{79}C_{15}B_6$, the reverse of what is happening in $Fe_{49}B_6C_{15}Mo_{14}Er_1Cr_{15}$. Note that $Fe_{49}B_6C_{15}Mo_{14}Er_1Cr_{15}$ can form 6 mm in diameter amorphous rods[26] whereas $Fe_{79}C_{15}B_6$ can only be made in ribbon form and is not entirely amorphous.

The local structure is built by extracting information on the atom topology and chemical environment from the model. For this the Voronoi tessellation technique[27,28] is

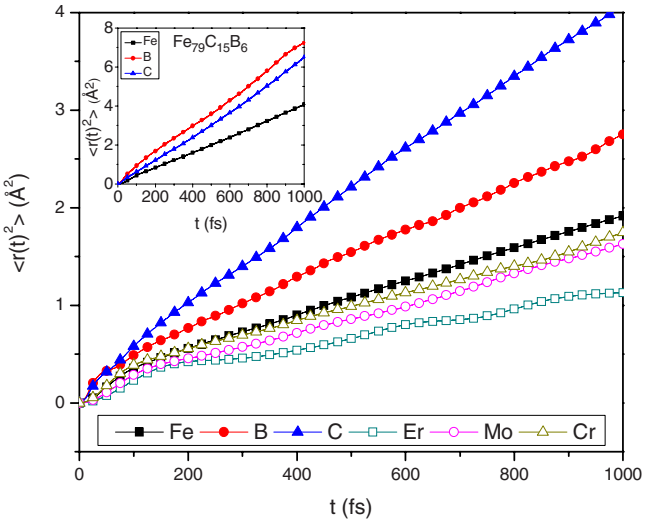

FIG. 2. (Color online) The mean-square displacements $\langle r(t)^2 \rangle$ of the different atom species in $Fe_{49}B_6C_{15}Mo_{14}Er_1Cr_{15}$ are plotted as a function of temperature. For comparison, $\langle r(t)^2 \rangle$ for the three atoms species of $Fe_{79}C_{15}B_6$ is shown in the inset.

used, where topological polygons that fill the three-dimensional space by phase sharing can be constructed. The Voronoi polyhedron corresponds to a region of space around an atom and all the points inside this region are closer to this atom than to any other atom. An example of three polygons that have the ME, TM, and RE ions as their centers is shown in Fig. 3(a). Note that the shape and volume around the same chemical element can be different, where the polygon size and number of facets increase with the size of the atom. In the case of crystals, such an analysis yields a small set of regular polyhedra. However, for glassy compounds, the number of different and irregular Voronoi polyhedra is quite large. For this reason, in order to determine the chemical coordination environments surrounding the ME, TM, and RE

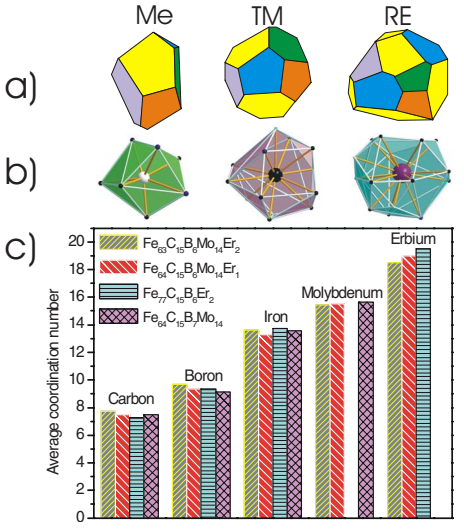

FIG. 3. (Color online) (a) Voronoi polyhedra with ME, TM, and RE as the central atoms. (b) The coordination polyhedra for the three central atoms. (c) The average coordination number of the three central atoms as a function of chemical composition.

TABLE I. List of chemical coordination environments for the first (from 0 to ~3 Å) and second coordination spheres (from ~3 to 5.7 Å) for the $Fe_{63}Er_2Mo_{14}C_{15}B_6$ alloy.

	Central atom				
	Fe	Mo	C	B	Er
	$1^{st}\|2^{nd}$	$1^{st}\|2^{nd}$	$1^{st}\|2^{nd}$	$1^{st}\|2^{nd}$	$1^{st}\|2^{nd}$
Fe	8.9‖34.0	9.8‖36.2	5.9‖35.6	6.8‖36.3	11.5‖36.5
Mo	2.2‖8.1	2.4‖6.4	1.4‖7.9	1.7‖7.7	2.2‖9.5
C	1.9‖9.2	1.6‖8.5	0.1‖8.8	0.7‖9.0	2.0‖8.0
B	0.7‖3.5	0.8‖3.3	0.3‖4.3	0.0‖3.4	1.5‖2.5
Er	0.3‖1.2	0.3‖1.4	0.3‖1.1	0.2‖0.8	0‖0

element groups, we considered the average distribution of coordination numbers from the entire set of Voronoi polygons. The coordination polyhedra around ME, TM, and RE are shown in Fig. 3(b) while the results from this analysis on four different alloys are depicted in the histogram in Fig. 3(c). It can be seen that the coordination of C is slightly smaller than for B while their coordination numbers are similar in all alloys shown between eight and nine. Fe has a coordination number of about 13 while the larger Mo has a coordination number of 15. As expected, Er has the highest coordination number of 18–19 because of its large atomic radius. The first coordination sphere depends on the size of the ion and the ratio of coordination to radius remains almost constant (~10.7 for C/B and ~10.6 for all other ions).

Such coordination polyhedra may serve as the building blocks for the local chemical order; they are the primary structural units of the glass. A detail list of the bond pair correlations within the first coordination sphere is provided in Table I for one of the alloys $Fe_{63}C_{15}B_6Mo_{14}Er_2$. These numbers vary from one alloy to the next, but they establish the general trend of atom-atom pair correlations. Bond pairs are listed for the second coordination sphere as well that can be used to describe the medium-range order. Given that the topological distribution of Voronoi polygons in the second coordination sphere increases considerably, there is no unique way to depict the medium-range structure.

Given the above structural models, the bulk modulus K is calculated in an effort to connect the atomic structure with the physical properties. K was calculated by first distorting a well-relaxed structure and then investigating the dependence of the energy on the volume. To estimate the error bars, the replica exchange method was used to generate nine different initial configurations for one composition and simultaneously relaxed all nine structures. A bulk modulus was then determined from the different structures from which the standard deviation was obtained. The standard deviation did not exceed 5% of the value of the bulk modulus for each of the nine different structures. K was calculated as a function of Er content and the values are compared with those obtained experimentally for three alloys of $Fe_{65-y}C_{15}B_6Mo_{14}Er_y$. The results are summarized in Table II. The experimental values were obtained from Ref. 29. Even though the change in chemical composition is quite small, the general trend of decreasing K with increasing Er content observed experimentally is correctly described by our theoretical approach—that in turn—shows that this technique is sensitive enough even with using a small model size. Small additions of RE atoms improve glass forming ability.[20,30] It has been suggested in Ref. 31 that RE ions can destabilize the formation of competing stable and metastable structures of Fe/Mo carbides and borides that easily form in the absence of RE. The slow diffusion of RE atoms demonstrated in Fig. 2 is not only due to a large atomic radius but mostly because RE atoms form structurally complex clusters that slow diffusion down for other chemical species, which may lead to better glass-forming ability.

To conclude, the computational and experimental approaches used in the study of multicomponent Fe glasses have proven quite useful in understanding structure-property relationships. Specifically, we have seen how short- and medium-range atomic clustering can play an important role in the diffusion and how short-range clusters persist well into the liquid state. At the same time, calculations of the bulk moduli reproduce the experimentally obtained values with very good accuracy. This shows that the volume is changed correctly in the model and the trends in K with Er concentration are reproduced.

The authors would like to acknowledge T. Proffen and P. Encinias of Los Alamos for their help with the NPD measurements and S. Short and J. Fieramosca of Argonne for their help with the SEPD measurements. We acknowledge valuable discussions with V. Sadtchenko and T. Egami. Support for this work was provided by a DARPA grant through the Office of Naval Research with Grant No. GG10799-31875 and the National Science Foundation through Grant No. 130398GA10715.

TABLE II. List of the bulk moduli determined experimentally are compared with the ones calculated using the *ab initio* MD simulation for $Fe_{65-y}Er_yMo_{14}C_{15}B_6$. The experimental values were obtained from Ref. 29. The standard deviation was determined to be six.

x (%)	0	1	2
K_{EXP}	195	178	177
$K_{THEO.}$	199	186	186

[1] *Bulk Metallic Glasses: An Overview*, edited by M. Miller, and P. Liaw (Springer, New York, 2007).
[2] P. Chaudhari and D. Turnbull, Science **199**, 11 (1978).
[3] A. Inoue, K. Ohtera, K. Kita, and T. Masumoto, Jpn. J. Appl. Phys., Part 2 **27**, L2248 (1988).
[4] A. Inoue, Mater. Trans., JIM **36**, 866 (1995).
[5] W. L. Johnson, Mater. Res. Bull. **24**, 42 (1999).
[6] T. C. Hufnagel and S. Brennan, Phys. Rev. B **67**, 014203 (2003).
[7] A. Hirata, Y. Hirotsu, T. Ohkubo, N. Tanaka, and T. G. Nieh, Intermetallics **14**, 903 (2006).
[8] R. L. McGreevy and P. Zetterstrom, J. Non-Cryst. Solids **293-295**, 297 (2001).
[9] G. Gutierrez and B. Johansson, Phys. Rev. B **65**, 104202 (2002).
[10] S. Blaineau, P. Jund, and D. A. Drabold, Phys. Rev. B **67**, 094204 (2003).
[11] B. E. Warren, *X-ray diffraction* (Dover, New York, 1990).
[12] T. Proffen, S. J. L. Billinge, T. Egami, and D. Louca, Z. Kristallogr. **218**, 132 (2003).
[13] V. Yu. Kazimirov, D. Louca, V. Ponnambalam, S. J. Poon, and T. Proffen, Phys. Rev. B **72**, 054207 (2005).
[14] K. Ahn, D. Louca, S. J. Poon, and G. J. Shiflet, Phys. Rev. B **70**, 224103 (2004).
[15] H. W. Sheng, W. K. Luo, F. M. Alamgir, J. M. Bai, and E. Ma, Nature (London) **439**, 419 (2006).
[16] H. W. Sheng, H. Z. Liu, Y. Q. Cheng, J. Wen, P. L. Lee, W. K. Luo, S. D. Shastri, and E. Ma, Nat. Mater. **6**, 192 (2007).
[17] E. M. Boczko and C. L. Brooks, Science **269**, 393 (1995).
[18] D. Kihara, H. Lu, A. Kolinski, and J. Skolnick, Proc. Natl. Acad. Sci. U.S.A. **98**, 10125 (2001).
[19] V. Ponnambalam, S. J. Poon, G. J. Shiflet, V. M. Keppens, R. Taylor, and G. Petculescu, Appl. Phys. Lett. **83**, 1131 (2003).
[20] V. Ponnambalam, S. J. Poon, and G. J. Shiflet, J. Mater. Res. **19**, 3046 (2004).
[21] B. H. Toby and T. Egami, Acta Crystallogr., Sect. A: Found. Crystallogr. **48**, 336 (1992).
[22] G. Kresse and J. Furthmuller, Comput. Mater. Sci. **6**, 15 (1996).
[23] H. J. Wang, K. Matsuda, S. Ikeno, S. J. Poon, and G. J. Shiflet, Appl. Phys. Lett. **91**, 141910 (2007).
[24] E. Matsubara, S. Sato, M. Imafuku, T. Nakamura, H. Koshiba, A. Inoue, and Y. Waseda, Mater. Sci. Eng., A **312**, 136 (2001).
[25] R. D. Shannon, Acta Crystallogr., Sect. A: Cryst. Phys., Diffr., Theor. Gen. Crystallogr. **32**, 751 (1976).
[26] X. J. Gu, S. J. Poon, and G. J. Shiflet, Scr. Mater. **57**, 289 (2007).
[27] J. L. Finney, Nature (London) **266**, 309 (1977).
[28] V. A. Borodin, Philos. Mag. A **79**, 309 (1999).
[29] X. J. Gu, A. G. McDermott, S. J. Poon, and G. J. Shiflet, Appl. Phys. Lett. **88**, 211905 (2006).
[30] Z. P. Lu, C. T. Liu, J. R. Thompson, and W. D. Porter, Phys. Rev. Lett. **92**, 245503 (2004).
[31] M. Mihalkovic and M. Widom, Phys. Rev. B **70**, 144107 (2004).